

This discussion paper is/has been under review for the journal Atmospheric Chemistry and Physics (ACP). Please refer to the corresponding final paper in ACP if available.

**Comprehensively
accounting for the
effect of giant CCN**

D. Barahona et al.

Comprehensively accounting for the effect of giant CCN in cloud droplet activation parameterizations

D. Barahona¹, R. E. L. West³, P. Stier³, S. Romakkaniemi⁴, H. Kokkola⁵, and A. Nenes^{1,2}

¹School of Chemical and Biomolecular Engineering, Georgia Institute of Technology, USA

²School of Earth and Atmospheric Sciences, Georgia Institute of Technology, USA

³Atmospheric, Oceanic and Planetary Physics, Department of Physics, University of Oxford, UK

⁴Department of Physics, University of Kuopio, Finland

⁵Finnish Meteorological Institute, Kuopio Unit, Finland

Received: 1 October 2009 – Accepted: 6 November 2009 – Published: 18 November 2009

Correspondence to: A. Nenes (athanasios.nenes@gatech.edu)

Published by Copernicus Publications on behalf of the European Geosciences Union.

Title Page

Abstract

Introduction

Conclusions

References

Tables

Figures

◀

▶

◀

▶

Back

Close

Full Screen / Esc

Printer-friendly Version

Interactive Discussion



Abstract

Cloud droplet activation parameterizations used in aerosol indirect effect assessments often assume that droplet growth after activation is much greater than their equilibrium size close to cloud base. This assumption does not hold for large CCN which may experience limited growth. If a large fraction of the aerosol is composed of such particles (such as regions with large fractions of dust particles and seasalt), neglecting such kinetic limitations in cloud droplet activation parameterizations leads to an underestimation of droplet surface area during cloud formation, hence overestimation of maximum supersaturation and cloud droplet number. Here we present a simple approach to address this problem and that can easily be incorporated into cloud droplet activation parameterizations. A demonstration of this method is done for activation parameterizations based on the “population splitting” concept of Nenes and Seinfeld (2003).

1 Introduction

Cloud droplet activation is the direct microphysical link between aerosol and clouds, and its accurate description is essential for studying aerosol indirect climate effects. Sophisticated parameterizations are currently used for describing activation in global circulation models (e.g., Feingold and Heymsfield, 1992; Abdul-Razzak and Ghan, 2000; Cohard et al., 2000; Nenes and Seinfeld, 2003; Fountoukis and Nenes, 2005; Ming et al., 2006), based on solutions to the coupled mass and energy balances in a Lagrangian parcel. Depending on the parameterization, effects of the aerosol composition (e.g., Abdul-Razzak and Ghan, 2000; Fountoukis and Nenes, 2005; Morrison and Grabowski, 2008), adsorption activation (Kumar et al., 2009), mixing and entrainment (Barahona and Nenes, 2007), and mass transfer limitations on droplet growth (Fountoukis and Nenes, 2005; Ming et al., 2006) can be accounted for.

Physically-based cloud droplet activation parameterizations usually neglect the size

Comprehensively accounting for the effect of giant CCN

D. Barahona et al.

Title Page

Abstract

Introduction

Conclusions

References

Tables

Figures

◀

▶

◀

▶

Back

Close

Full Screen / Esc

Printer-friendly Version

Interactive Discussion



of droplets at cloud base on the basis that droplet size after activation is substantially increased (e.g., Twomey, 1959; Abdul-Razzak and Ghan, 2000; Nenes and Seinfeld, 2003). This assumption works well in the majority of atmospherically-relevant conditions of droplet formation, but may introduce error when the “inertial mechanism” affects a large fraction of the CCN population (Chuang et al., 1997; Nenes et al., 2001). The inertial mechanism is a kinetic limitation that precludes aerosol particles from reaching their equilibrium size. It arises when aerosol particles do not grow fast enough to follow changes in supersaturation and equilibrium diameter (Chuang et al., 1997). Thus, inertially-limited particles, although having very low critical supersaturation (and therefore a positive driving force for condensation), cannot attain their critical size within the timescale typically associated with CCN activation in clouds. The wet diameter of these particles around saturation is of order $1\ \mu\text{m}$, hence the liquid water content and surface area of these particles may be comparable to that from strictly activated droplets (i.e., those particles with a wet size larger than the critical diameter of their equilibrium curve), particularly in polluted clouds where the supersaturation is very low (Charlson et al., 2001). Incorrectly accounting for this surface area can underestimate the condensation rate of water vapor, which leads to overestimation in maximum supersaturation, s_{max} , and droplet number (e.g., Barahona and Nenes, 2007; Kumar et al., 2008). For single-mode aerosol, an overestimation of s_{max} may not lead to substantial errors in droplet number, given that most CCN would activate (e.g., Nenes et al., 2001; Barahona and Nenes, 2007; Kumar et al., 2008). This may not be the case for multimodal aerosol (particularly those with a prominent nucleation mode), as a positive bias in s_{max} may erroneously activate a substantial number of small particles.

Including the contribution of inertially-limited CCN in the water vapor balance equation (required for computation of supersaturation) is challenging. Nenes and Seinfeld (2003) used the concept of “population splitting” to differentiate between particles that activate and those that are inertially-limited; the approach of Twomey (1959) is used for the former which works for most cases, but breaks down when a significant fraction of large CCN is present. Ming et al. (2006) proposed the usage of a semi-empirical power

**Comprehensively
accounting for the
effect of giant CCN**

D. Barahona et al.

Title Page

Abstract

Introduction

Conclusions

References

Tables

Figures

◀

▶

◀

▶

Back

Close

Full Screen / Esc

Printer-friendly Version

Interactive Discussion



law to express growth, but a application of this approach in existing parameterization frameworks may not be straightforward. In this work, a different approach is proposed, in which the condensation surface area from inertially-limited droplets is considered in the water vapor balance equations. The application of this method does not require reformulation of a parameterization, and is illustrated using the parameterizations of Nenes and Seinfeld (2003) and Fountoukis and Nenes (2005).

2 Development of the inertial effect correction

Every physically-based droplet formation parameterization conceptually consists of two steps, one involving the determination of the “CCN spectrum” (i.e., the number of CCN that can activate at a given level of supersaturation computed by Köhler or adsorption activation theory) and one determining the maximum supersaturation, s_{\max} , that develops in the ascending parcel. The droplet number concentration is then just the value of the CCN spectrum at s_{\max} . Supersaturation in the ascending parcel is determined from (Seinfeld and Pandis, 1998; Nenes and Seinfeld, 2003; Barahona and Nenes, 2007),

$$\frac{ds}{dt} = \alpha V \left(1 - \frac{e}{e_c}\right) - \gamma \frac{dW}{dt} \quad (1)$$

where $\frac{dW}{dt}$ is the rate of condensation of liquid water onto the drops, V is the updraft velocity, e is the fractional entrainment rate (if mixing effects are negligible then $e=0$), $e_c \approx \alpha \left[(1-RH) - \frac{\Delta H_v M_w}{RT^2} (T-T') \right]^{-1}$, is the critical entrainment rate (Barahona and Nenes, 2007), $\alpha = \frac{g M_w \Delta H_v}{c_p R T^2} - \frac{g M_a}{RT}$, $\gamma = \frac{\rho M_a}{\rho^s(T) M_w} + \frac{M_w \Delta H_v^2}{c_p R T^2}$, ΔH_v is the latent heat of vaporization of water, g is the acceleration of gravity, T and T' are the parcel and ambient temperature, respectively, RH is the ambient relative humidity, c_p is the heat capacity of air, $\rho^s(T)$ is the water saturation vapor pressure (over a flat surface) at T , p is the ambient pressure, M_w and M_a are the molar masses of water and air, respectively, and R is the universal

Title Page

Abstract

Introduction

Conclusions

References

Tables

Figures

◀

▶

◀

▶

Back

Close

Full Screen / Esc

Printer-friendly Version

Interactive Discussion



gas constant. The maximum supersaturation, s_{\max} , is found from Eq. (1) by setting $\frac{ds}{dt}=0$.

When large CCN are not affecting droplet number, $\frac{dW}{dt}$ at the point of maximum supersaturation in the cloud ascent is symbolized as $\frac{dW}{dt}\Big|_{ps}$ and computed using the parameterization of interest. When inertially-limited CCN dominate $\frac{dW}{dt}$, then droplets do not substantially change size from cloud base to the level of s_{\max} ; the condensation rate in this limit is represented as $\frac{dW}{dt}\Big|_{ie}$. When both activated and inertially-limited CCN contribute to condensation, $\frac{dW}{dt}$ at the point of maximum supersaturation can be written as

$$\frac{dW}{dt} = \frac{dW}{dt}\Big|_{ie} + \frac{dW}{dt}\Big|_{ps} \quad (2)$$

$\frac{dW}{dt}\Big|_{ie}$ can be computed from the liquid water content at cloud base in equilibrium with the aerosol particles that would eventually become droplets, i.e.,

$$W|_{ie} = \frac{\pi \rho_w}{6 \rho_a} \left[\int_{\ln D_{p\min}}^{\infty} D_p^3 n(\ln D_p) d \ln D_p \right] \quad (3)$$

where $n(D_p)$ is the droplet size distribution, and D_p is their size at saturation, given by Köhler theory (Seinfeld and Pandis, 1998),

$$D_p = \frac{2}{3\sqrt{3}} \frac{A}{s_c} \quad (4)$$

where $A = \frac{4\sigma M_w}{RT\rho_w}$, σ is the surface tension of the droplet at saturation, and s_c is the droplet critical supersaturation. $D_{p\min}$ in Eq. (3) is the equilibrium diameter, at saturation, of the smallest particle that activates (i.e., for which $s_c = s_{\max}$), i.e., $D_{p\min} = \frac{2}{3\sqrt{3}} \frac{A}{s_{\max}}$.

Comprehensively accounting for the effect of giant CCN

D. Barahona et al.

Title Page

Abstract

Introduction

Conclusions

References

Tables

Figures

◀

▶

◀

▶

Back

Close

Full Screen / Esc

Printer-friendly Version

Interactive Discussion



$\frac{dW}{dt} \Big|_{ie}$ is calculated taking the derivative of Eq. (3), assuming that the droplet diameter does not change between cloud base and s_{\max} , and $\frac{dD_p}{dt} = \frac{Gs}{D_p}$ (Seinfeld and Pandis, 1998)

$$\frac{dW}{dt} \Big|_{ie} = \frac{\pi \rho_w}{2 \rho_a} Gs \left[\int_{\ln D_{p\min}}^{\infty} D_p n(\ln D_p) d \ln D_p \right] \quad (5)$$

5 with

$$G = \frac{4}{\frac{\rho_w RT}{\rho^s(T) D'_v M_w} + \frac{\Delta H_v \rho_w}{k_a T} \left(\frac{\Delta H_v M_w}{RT} - 1 \right)} \quad (6)$$

where k_a is the thermal conductivity of air, D'_v is the water vapor mass transfer coefficient from the gas to the droplet phase corrected for non-continuum effects, computed as suggested by Fountoukis and Nenes (2005).

10 2.1 Calculating the wet size distribution of inertially-limited CCN

Using Köhler theory (Seinfeld and Pandis, 1998) the equilibrium size, at saturation (i.e., $s=0$), of a particle with dry size d_s , is given by

$$D_p = \left(\frac{B}{A} \right)^{1/2} d_s^{3/2} \quad (7)$$

15 where $B = \frac{\nu M_w \rho_s}{M_s \rho_w}$, and ν is the effective van't Hoff factor. Using Eq. (7), the wet size distribution at saturation can be expressed in terms of the dry size distribution as

$$n(\ln D_p) = \frac{dN_d}{d \ln D_p} = \frac{dN_d}{d \ln d_s} \frac{d \ln d_s}{d \ln D_p} = \frac{2}{3} \frac{dN_d}{d \ln d_s} \quad (8)$$

where N_d is the droplet number concentration.

**Comprehensively
accounting for the
effect of giant CCN**

D. Barahona et al.

Title Page

Abstract

Introduction

Conclusions

References

Tables

Figures

◀

▶

◀

▶

Back

Close

Full Screen / Esc

Printer-friendly Version

Interactive Discussion



For a lognormal aerosol representation,

$$\frac{dN_a}{d\ln d_s} = \sum_{i=1}^{n_m} \frac{N_i}{\sqrt{2\pi}\ln\sigma_i} \exp\left[-\frac{\ln^2(d_s/d_{g,i})}{2\ln^2\sigma_i}\right] \quad (9)$$

where $d_{g,i}$, σ_i are the geometric mean diameter and the geometric standard deviation of mode i , respectively, n_m is the number of lognormal modes, N_a the total aerosol concentration, and N_i is the aerosol concentration of mode i . Substituting Eqs. (7) and (8) into Eq. (9) gives

$$\frac{dN_d}{d\ln D_p} = \sum_{i=1}^{n_m} \frac{2}{3} \frac{N_i}{\sqrt{2\pi}\ln\sigma_i} \exp\left[-\frac{4}{9} \frac{\ln^2(D_p/D_{g,i})}{2\ln^2\sigma_i}\right] \quad (10)$$

where $D_{g,i}$ is the equilibrium size of $d_{g,i}$ at saturation given by Eq. (7). Substitution of Eq. (10) into Eq. (5) gives the condensation rate of inertially limited CCN at s_{\max} ,

$$\frac{dW}{dt} \Big|_{ie} = \frac{\pi}{2} \frac{\rho_w}{\rho_a} G s_{\max} \sum_{i=1}^{n_m} \frac{N_i}{2} D_{g,i} \exp\left(\frac{9}{8} \ln^2\sigma_i\right) \operatorname{erfc}\left[\frac{2}{3\sqrt{2}} \frac{\ln(D_{p\min}/D_{g,i})}{\ln\sigma_i} - \frac{3}{2\sqrt{2}} \ln\sigma_i\right] \quad (11)$$

Using Eq. (5), Eq. (11) can be written in terms of the mean droplet diameter

$$\bar{D}_p = \frac{1}{N_d} \int_{\ln D_{p\min}}^{\infty} D_p n(\ln D_p) d\ln D_p, \text{ as}$$

$$\frac{dW}{dt} \Big|_{ie} = \frac{\pi}{2} \frac{\rho_w}{\rho_a} G s_{\max} N_d \bar{D}_p. \quad (12)$$

For a sectional aerosol representation,

$$\frac{dN_d}{d\ln d_s} = \frac{\Delta N_m}{\Delta \ln d_{s,m}} = \frac{\Delta N_m}{\ln d_{s,m} - \ln d_{s,m-1}} \quad (13)$$

Title Page

Abstract

Introduction

Conclusions

References

Tables

Figures

◀

▶

◀

▶

Back

Close

Full Screen / Esc

Printer-friendly Version

Interactive Discussion



where ΔN_m is the number concentration of particles in section m , and, $d_{s,m}$ and $d_{s,m-1}$ are the “upper” and “lower” dry diameters of the section m , respectively (Nenes and Seinfeld, 2003). Substituting Eqs. (7) and (8) into (13) gives

$$\frac{dN_d}{d\ln D_p} = \frac{\Delta N_m}{\Delta \ln D_{p,m}} = \frac{\Delta N_m}{\ln D_{p,m} - \ln D_{p,m-1}} \quad (14)$$

5 where $D_{p,m}$ and $D_{p,m-1}$ are the droplet diameters in equilibrium with $d_{s,m}$ and $d_{s,m-1}$, respectively. Substitution of Eq. (14) into Eq. (5) gives,

$$\left. \frac{dW}{dt} \right|_{ie} = \frac{\pi \rho_w}{2 \rho_a} G s_{\max} \sum_{m=i_{\max}}^{n_{\text{sec}}} D_{p,m} \frac{\Delta N_m}{\Delta \ln D_{p,m}} \Delta \ln D_{p,m} \quad (15)$$

where n_{sec} is the total number of sections and $D_{p,m}$ is averaged within section m , and i_{\max} is the section that contains s_{\max} . Defining the average droplet diameter at the limit

10 where all are inertially limited as $\bar{D}_p = \frac{1}{N_d} \sum_{m=i_{\max}}^{n_{\text{sec}}} D_{p,m} \frac{\Delta N_m}{\Delta \ln D_{p,m}} \Delta \ln D_{p,m}$, the condensation

rate $\left. \frac{dW}{dt} \right|_{ie}$ for sectional aerosol can also be expressed in the form of Eq. (12). The following section provides an example for the Nenes and Seinfeld (2003) activation parameterization.

3 Comprehensively implementing inertially-limited CCN effects: demonstration for “population splitting” activation frameworks

15 Using the “population splitting” approach of Nenes and Seinfeld (2003), $\left. \frac{dW}{dt} \right|_{ps}$ at s_{\max} can be written as the sum of two terms,

$$\left. \frac{dW}{dt} \right|_{ps} = \frac{\pi \rho_w}{2 \rho_a} G s_{\max} [I_1(0, s_{\text{part}}) + I_2(s_{\text{part}}, s_{\max})] \quad (16)$$

Title Page

Abstract

Introduction

Conclusions

References

Tables

Figures

◀

▶

◀

▶

Back

Close

Full Screen / Esc

Printer-friendly Version

Interactive Discussion



Comprehensively accounting for the effect of giant CCN

D. Barahona et al.

Title Page

Abstract

Introduction

Conclusions

References

Tables

Figures

◀

▶

◀

▶

Back

Close

Full Screen / Esc

Printer-friendly Version

Interactive Discussion



The functions $I_1(0, s_{\text{part}})$ and $I_2(s_{\text{part}}, s_{\text{max}})$ are given in Nenes and Seinfeld (2003) and Fountoukis and Nenes (2005) for sectional and lognormal aerosol representations, respectively. The partition supersaturation, s_{part} , separates two CCN populations, one (expressed by I_2) for which droplets experience negligible growth beyond the critical diameter ($s_c \approx s_{\text{max}}$), and one (expressed as I_1) for which droplet growth is much larger than the critical diameter ($s_c \ll s_{\text{max}}$). In reality, the large inertially limited CCN is a third population, as they have low s_c , but do not reach their critical diameter at the point of s_{max} . Nenes and Seinfeld (2003) recognized this, and postulated (guided by numerical simulations) that the growth experienced by these particles is still substantially larger than their dry diameter, hence can be approximated with I_1 . This approximation may not apply for very large and giant CCN, so that a third term, $\frac{dW}{dt} \Big|_{ie}$, must be added to Eq. (16) to account for their effect on the condensation rate. Combining Eqs. (16), (2), and Eq. (12) gives for the supersaturation balance at s_{max} :

$$\frac{\frac{\pi}{2} \frac{\rho_w}{\rho_a} G s_{\text{max}}}{\frac{\alpha V}{\gamma} \left(1 - \frac{e}{e_c}\right)} \left\{ I_1(0, s_{\text{part}}) + I_2(s_{\text{part}}, s_{\text{max}}) + N_a \bar{D}_\rho \Big|_{s_{\text{part}}} \right\} - 1 = 0 \quad (17)$$

$\bar{D}_\rho \Big|_{s_{\text{part}}}$ is calculated at s_{part} instead of s_{max} (i.e., $D_{\rho \text{min}} = \frac{2}{3\sqrt{3}} \frac{A}{s_{\text{part}}}$ in Eqs. 11 and 15). This is justified as s_{part} represents the limit between particles that experienced significant growth after activation and those that are inertially limited (Nenes and Seinfeld, 2003). Thus, $I_2(s_{\text{part}}, s_{\text{max}})$ is calculated assuming that droplets do not grow substantially beyond their size at s_{part} . Equation (17) is solved iteratively to find s_{max} and cloud droplet number concentration is calculated from the cumulative CCN spectrum, $F^S(s)$, at s_{max} , (Nenes and Seinfeld, 2003).

4 Comparison against parcel model results

The modified parameterization is evaluated by comparing predictions of s_{max} and droplet number against simulations with a comprehensive cloud parcel model (Nenes

Comprehensively accounting for the effect of giant CCN

D. Barahona et al.

Title Page

Abstract

Introduction

Conclusions

References

Tables

Figures

◀

▶

◀

▶

Back

Close

Full Screen / Esc

Printer-friendly Version

Interactive Discussion



et al., 2001) for a wide range of updraft velocity and aerosol size distribution characteristics. Initial parcel temperature and pressure were 290 K and 100 kPa, respectively, and the water uptake coefficient was set to 0.06, following the suggestions of Fountoukis et al. (2007). Entrainment effects were not considered ($e=0$). The aerosol was assumed to be pure ammonium sulfate and composed of two lognormal modes, with number concentration $N_1=2000\text{ cm}^{-3}$ and $N_2=400\text{ cm}^{-3}$, respectively. The geometric dispersion for both modes is set to $\sigma_1=\sigma_2=1.59$; $d_{g,1}$ was set to $0.08\text{ }\mu\text{m}$. These values were selected as representative of atmospheric aerosol (Seinfeld and Pandis, 1998). V was varied over conditions expected in GCM simulations (0.01 to 10 m s^{-1}), and $d_{g,2}$ was varied between 0.005 and $5\text{ }\mu\text{m}$ to represent typical values of recently nucleated particles ($<0.01\text{ }\mu\text{m}$) and dust and giant CCN ($>1\text{ }\mu\text{m}$) (Pruppacher and Klett, 1997).

Parcel model results indicate that at high V ($>5\text{ m s}^{-1}$) and moderate $d_{g,2}$ ($\sim 0.1\text{ }\mu\text{m}$) the activation fraction reaches high values, as the s_{max} is sufficiently high ($\sim 1\%$) to activate most CCN. However as $d_{g,2}$ increases, significant water vapor depletion by droplets in the second mode decreases s_{max} , therefore reducing the activation fraction (as fewer particles from the first mode activate). As $d_{g,2}$ becomes substantially large ($>0.5\text{ }\mu\text{m}$), the activation fraction approaches 16% as all particles of the second mode are activated (i.e., they have $s_c < s_{\text{max}}$) and a negligible fraction of the first mode activate. At this limit underestimating the surface area from large CCN overpredicts s_{max} and the activation fraction hence the droplet concentration, especially for $d_{g,2} > 0.5\text{ }\mu\text{m}$ (Fig. 1). Accounting for depletion effects from inertially-limited CCN largely corrects this bias (Eq. 17) producing results that are in agreement with the parcel model. Figure 1 shows that for $d_{g,2} > 0.5\text{ }\mu\text{m}$, significant deviations between the parameterization and the parcel model occur; which are to a large extent reduced at lower $d_{g,2}$. For $d_{g,2} > 0.5\text{ }\mu\text{m}$ applying the correction for large CCN, significantly reduces the difference in s_{max} between the parameterization and the parcel model.

Sensitivity tests were run using the parcel model for $d_{g,2}=0.12\text{ }\mu\text{m}$, varying N_2 between 50 and $5\times 10^4\text{ cm}^{-3}$. All other conditions were maintained as in Fig. 1. At low $N_2 \sim 100\text{ cm}^{-3}$, an increase in the activation fraction from 10% to 80% was produced

**Comprehensively
accounting for the
effect of giant CCN**

D. Barahona et al.

Title Page

Abstract

Introduction

Conclusions

References

Tables

Figures

◀

▶

◀

▶

Back

Close

Full Screen / Esc

Printer-friendly Version

Interactive Discussion

when V increased from 0.1 to 1 m s⁻¹; at high $N_2 > 10^4$ cm⁻³, significant activation fractions were found only for $V > 0.5$ m s⁻¹. At these conditions however the effect of large CCN was not significant and the Nenes and Seinfeld (2003) parameterization reproduced the results of the parcel model. Accounting for the effect of kinetic limited CCN produced a lower activation fraction at high N_2 but mostly within 10% of the values obtained without the correction. This is expected, as surface area of the aerosol particles at cloud base is negligible compared to the surface area of activated droplets; thus, significant droplet growth after activation occurs, and the equilibrium size at cloud base is negligible compared to the size after activation. A second sensitivity test was carried out for $d_{g,2} = 0.12$ μm and $N_2 = 400$ cm⁻³ and varying σ_2 between 1.05 and 5.0 (all other conditions as before). Results show that the effect of inertially limited CCN for $\sigma_2 > 2.5$ significantly reduced the activated fraction (compared to neglecting such effects), since a substantial fraction of aerosol are giant CCN. In both sensitivity tests, the effects of inertially limited CCN were much more pronounced when $d_{g,2}$ was increased to values over 0.5 μm, which is also evident in Fig. 1.

The assessment was repeated using the lognormal aerosol activation parameterization of Fountoukis and Nenes (2005), using Eq. (11) to calculate $\bar{D}_p |_{s_{part}}$; the calculated activated fraction was within 1% of the results using the sectional formulation of Nenes and Seinfeld (2003). Finally, for the runs presented in Fig. 1, including the correction for inertially limited CCN increased computational time by about 2% and 7% for the sectional and lognormal and versions of the parameterization, respectively.

5 Conclusions

When a significant fraction of large CCN are present during cloud formation (i.e. droplets which at the point of maximum supersaturation in a cloud updraft have not experienced significant growth compared to cloud base), their contribution to the droplet surface area must be accounted for to avoid biases in maximum supersaturation and

droplet number. A general correction is proposed for droplet activation parameterizations, where the condensation upon inertially-limited droplets is added to the “default” expression in the parameterization of interest. The correction was incorporated into the Nenes and Seinfeld (2003) and Fountoukis and Nenes (2005) parameterizations and tested for wide range of conditions. Results show that incorporation of the correction greatly improved the parameterization performance for conditions where inertially-limited CCN dominate droplet formation, without significant impact on the computational burden of the parameterization. The approach outlined here can easily be extended to include adsorption activation of mineral dust (Kumar et al., 2009), and, the water vapor depletion from preexisting droplets during secondary activation events in convective updrafts.

Acknowledgements. This study was supported by NASA ACPMAP, and a NASA New Investigator Award. Rosalynd West was supported by a NERC studentship and a CASE award from the UK Met Office. S. Romakkaniemi was funded by the Academy of Finland (decision number 123466).

References

- Abdul-Razzak, H. and Ghan, S.: A parameterization of aerosol activation, 2. Multiple aerosol types, *J. Geophys. Res.*, 105, 6837–6844, doi:6810.1029/1999JD901161, 2000.
- Barahona, D. and Nenes, A.: Parameterization of cloud droplet formation in large scale models: including effects of entrainment, *J. Geophys. Res.*, *J. Geophys. Res.*, 112, D16206, doi:10.1029/2007JD008473, 2007.
- Charlson, R. J., Seinfeld, J. H., Nenes, A., Kulmala, M., Laaksonen, A., and Facchini, M. C.: Reshaping the theory of cloud formation, *Science*, 292, 2025–2026, 2001.
- Chuang, P. Y., Charlson, R. J., and Seinfeld, J. H.: Kinetic limitations on droplet formation in clouds, *Nature*, 390, 594–596, 1997.
- Cohard, J.-M., Pinty, J.-P., and Suhre, K.: On the parameterization of activation spectra from cloud condensation nuclei microphysical properties, *J. Geophys. Res.*, 105, 11753–11766, doi:11710.11029/11999JD901195, 2000.

Comprehensively accounting for the effect of giant CCN

D. Barahona et al.

Title Page

Abstract

Introduction

Conclusions

References

Tables

Figures

◀

▶

◀

▶

Back

Close

Full Screen / Esc

Printer-friendly Version

Interactive Discussion



**Comprehensively
accounting for the
effect of giant CCN**

D. Barahona et al.

Title Page

Abstract

Introduction

Conclusions

References

Tables

Figures

◀

▶

◀

▶

Back

Close

Full Screen / Esc

Printer-friendly Version

Interactive Discussion

Feingold, G. and Heymsfield, A. J.: Parameterization of condensational growth of droplets for use in general circulation models, *J. Atmos. Sci.*, 49, 2325–2342, 1992.

Fountoukis, C. and Nenes, A.: Continued development of a cloud droplet formation parameterization for global climate models, *J. Geophys. Res.*, 110, D11212, doi:10.1029/12004JD005591, 2005.

Kumar, P., Sokolik, I. N., and Nenes, A.: Parameterization of cloud droplet formation for global and regional models: including adsorption activation from insoluble CCN, *Atmos. Chem. Phys.*, 9, 2517–2532, 2009, <http://www.atmos-chem-phys.net/9/2517/2009/>.

Ming, Y., Ramaswamy, V., Donner, L. J., and Phillips, V. T. J.: A new parameterization of cloud droplet activation applicable to general circulation models, *J. Atmos. Sci.*, 63, 1348–1356, 2006.

Morrison, H. and Grabowski, W.: Modeling supersaturation and subgrid-scale mixing with two-moment bulk warm microphysics, *J. Atmos. Sci.*, 65, 792–812, 2008.

Nenes, A., Ghan, S., Abdul-Razzak, H., Chuang, P. Y., and Seinfeld, J. H.: Kinetic limitations on cloud droplet formation and impact on cloud albedo, *Tellus*, 53B, 133–149, 2001.

Nenes, A. and Seinfeld, J. H.: Parameterization of cloud droplet formation in global climate models, *J. Geophys. Res.*, 108, 4415, doi:10.1029/2002JD002911, 2003.

Pruppacher, H. R. and Klett, J. D.: *Microphysics of clouds and precipitation* 2nd edn., Kluwer Academic Publishers, Boston, MA, 954 pp., 1997.

Seinfeld, J. H. and Pandis, S. N.: *Atmospheric Chemistry and Physics*, John Wiley and Sons, New York, NY, USA, 1998.

Twomey, S.: The nuclei of natural cloud formation. II. The supersaturation in natural clouds and the variation of cloud droplet number concentration, *Pure Appl. Geophys.*, 43, 243–249, doi:10.1007/BF01993560, 1959.

Comprehensively
accounting for the
effect of giant CCN

D. Barahona et al.

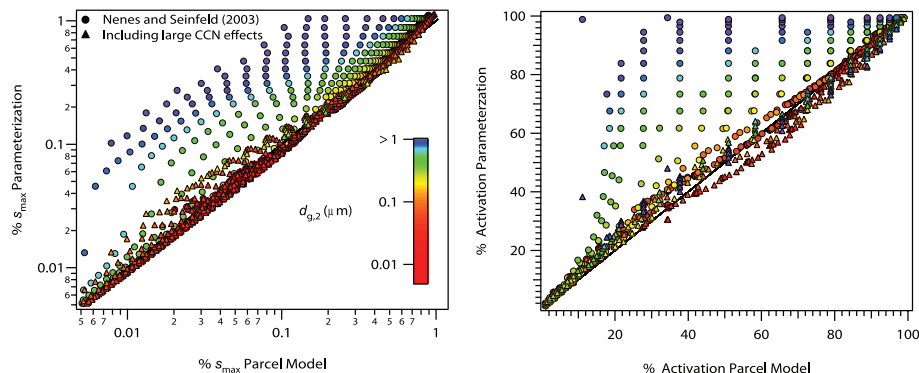


Fig. 1. Aerosol activation fraction (right) and maximum supersaturation (left) for a bimodal aerosol distribution. Results from the Nenes and Seinfeld (2003) parameterization neglecting aerosol distribution are presented (circles) and considering (triangles) the effect of kinetic limitations on large CCN are presented. Conditions considered are $N_1=2000\text{ cm}^{-3}$ and $N_2=400\text{ cm}^{-3}$, $\sigma_1=\sigma_2=1.59$, $d_{g,1}=0.08\text{ }\mu\text{m}$, $T=290\text{ K}$, $p=100\text{ kPa}$, and $\alpha_c=0.06$. Symbols with the same color vary with updraft speed.

Title Page

Abstract

Introduction

Conclusions

References

Tables

Figures

◀

▶

◀

▶

Back

Close

Full Screen / Esc

Printer-friendly Version

Interactive Discussion

